Head and Neck Pathol (2015) 9:85–95
DOI 10.1007/s12105-014-0557-1

ORIGINAL PAPER

Morphology in Conjunction with Immunohistochemistry is Sufficient for the Diagnosis of Mammary Analogue Secretory Carcinoma

Akeesha A. Shah · Bruce M. Wenig · Robin D. LeGallo · Stacey E. Mills · Edward B. Stelow

Received: 16 May 2014 / Accepted: 2 July 2014 / Published online: 31 July 2014

Abstract The recently described mammary analogue secretory carcinoma (MASC) is a low-grade salivary gland malignancy that harbors the recurrent cytogenetic abnormality t(12;15) (p13;q25) *ETV6-NTRK3*. Confirmation of this is currently considered the gold standard for diagnosis. Some have postulated that morphology together with supporting immunohistochemistry is sufficient to diagnose MASC. In this study we retrospectively review a series of 19 MASCs diagnosed based on histology in conjunction with immunohistochemistry; subsequently we performed in situ hybridization using an *ETV6* break-apart probe. Immunohistochemistry for S100 protein and mammaglobin as well as fluorescence in situ hybridization using the Vysis *ETV6* Dual Color Break-Apart FISH Probe Kit were performed on all cases. The 19 cases were from 12 females and 7 males with ages ranging from 16 to 76 years (mean = 45 years). Sixteen cases were from the parotid gland, 1 case was from a periparotid lymph node and 2 cases were from the submandibular gland. All 19 cases demonstrated moderate to strong expression of S100 protein. Eighteen cases demonstrated strong, diffuse expression of mammaglobin, while one case had only rare tumor cells that strongly expressed mammaglobin. Eighteen of 19 cases (95 %) demonstrated the *ETV6* rearrangement by fluorescence in situ hybridization. Given that morphology together with immunohistochemistry is highly correlated with the *ETV6* gene rearrangement, we conclude that molecular confirmation is not required to diagnose MASC.

Keywords Mammary analogue secretory carcinoma · Salivary gland · ETV6 · Fluorescence in situ hybridization · Immunohistochemistry · Mammaglobin

A. A. Shah · R. D. LeGallo · S. E. Mills · E. B. Stelow (✉)
Department of Pathology, University of Virginia Health System, 1215 Lee St., MC, 800214, Jefferson Park Ave., Charlottesville, VA 22908, USA
e-mail: es7yj@virginia.edu

B. M. Wenig
Department of Pathology, Mount Sinai Health System-Beth Israel Medical Center, First Avenue at 16th Street, Silver 11; Room 34, New York, NY 10003, USA

Introduction

Mammary analogue secretory carcinoma (MASC) was first described by Skalova et al. [1] in 2010. Implicit in its name, the tumor is morphologically, immunohistochemically and molecularly akin to secretory carcinoma of the breast [1]. Both tumors have the t(12;15) (p13;q25) translocation which creates the *ETV6-NTRK3* fusion gene [1, 2]. This fusion gene has also been detected in congenital fibrosarcoma, the cellular variant of congenital mesoblastic nephroma and rare cases of acute myelogenous leukemia [3–7]. While secretory carcinoma of the breast is a rare carcinoma subtype, the incidence of MASC is yet unknown. In our shared experience at two tertiary academic institutions (University of Virginia and Mount Sinai Health System-Beth Israel Medical Center), both with moderately sized consultation practices, we see a fair number of these tumors each year. These cases are often referred to us with a preliminary diagnosis of acinic cell carcinoma, salivary duct carcinoma and adenocarcinoma not otherwise specified. However, in the past year many of our referral pathologists have correctly suggested the diagnosis of MASC, sending the case for diagnostic confirmation.

There are a handful of salivary gland tumors that have been demonstrated to have recurring cytogenetic abnormalities

including adenoid cystic carcinomas [t(6;9) (*MYB-NFIB*)] [8–10], mucoepidermoid carcinomas [t(11:19) (*MECT1-MAML2*)] [11, 12], pleomorphic adenomas (*PLAG1* and *HMGA2* rearrangements) [13–17], and hyalinizing clear cell carcinoma [t(12;22) (*EWSR1-ATF*)] [18, 19]. In the majority of these tumors, the morphology is distinctive enough to allow for a diagnosis and molecular confirmation is typically not necessary. Currently, molecular confirmation is considered the gold standard for the diagnosis of MASC. However, we postulate that the features as described by Skalova et al. [1] in conjunction with the appropriate immunohistochemical profile are sufficient for a diagnosis of MASC in virtually all cases. In order to test this hypothesis, we retrospectively reviewed a series of tumors originally diagnosed as MASC based on histologic and immunohistochemical findings and subsequently performed fluorescence in situ hybridization for *ETV6*.

Materials and Methods

A natural language search was performed to identify MASCs using two institution's anatomic pathology laboratory information systems. Search terms included "secretory carcinoma" in the final diagnosis or diagnosis comment; all cases selected were from the head and neck location. Eleven cases (10 consultation and 1 in-house) were retrieved from the files of the University of Virginia between October 2010 and February 2014. Nine additional MASCs, also representing consultation cases were obtained from the Mount Sinai Health System—Beth Israel Medical Center.

The histopathologic features of all tumors and the accompanying immunohistochemical stains when available were reviewed by two pathologists (E.B.S and A.A.S). A diagnosis of MASC was confirmed in cases that displayed the histologic features as described by Skalova et al. [1] and in cases in which there was a supporting immunohistochemical profile, i.e., co-expression of S100 protein and mammaglobin. Upon review of the 20 cases, the diagnosis of MASC was retained in 19 tumors; 1 parotid gland tumor was reclassified as a low-grade cribriform cystadenocarcinoma also known as low-grade salivary duct carcinoma and intraductal carcinoma.

Histologic features used to aid in a diagnosis of MASC included a variety of architectural growth patterns including microcystic, macrocystic, solid, tubular, papillary and pseudopapillary growth. Light pink to colloid-like secretions were also frequently seen. Neoplastic cells had to have oval to round nuclei with vesicular to finely granular chromatin, frequently with a single, distinct nucleolus. The tumor cells were also required to have eosinophilic cytoplasm with varying degrees of vacuolation.

If S100 protein and mammaglobin immunohistochemistry were not performed by the referring institution, then these immunohistochemical stains were performed either at the University of Virginia or at the Mount Sinai Health System-Beth Israel Medical Center. Immunohistochemical staining for DOG1, a newly described marker for acinic cell carcinoma, was also performed in tumors that were negative for the *ETV6* rearrangement [20]. Immunohistochemistry was performed on 4-μm-thick sections from formalin-fixed paraffin-embedded tissue. The University of Virginia utilized the Dako EnVision Plus Dual Link System-Horseradish Peroxidase technique with commercially purchased antibodies against S100 protein (polyclonal rabbit, 1:16,000 dilution, Dako) and mammaglobin cocktail (304-1A5 & 31A5 clones, 1:50 dilutions, Dako); staining was performed in a Dako Autostainer Plus (Dako North America Inc., Carpinteria, CA). Beginning in March 2013, immunohistochemical stains at the University of Virginia were performed with ready-to-use (RTU) commercially purchased antibodies performed in a Dako Envision Flex Detection system. Immunohistochemistry at the Mount Sinai Health System-Beth Israel Medical Center was performed in a Leica BOND III Autostainer (Leica Microsystems, Melborne, Australia) using the Leica Bond Polymer Refine Detection System with the following commercially purchased antibodies: S100 protein (polyclonal rabbit, RTU, Leica), mammaglobin (Monocloan C5/D5, 1: 1:200 dilution, Cell Marque) and DOG1 (K9 clone, RTU, Leica).

FISH for the *ETV6* rearrangement was performed on whole-mount unstained sections for all 19 MASCs and the single low-grade cribriform cystadenocarcinoma. Four-μm-thick sections of formalin-fixed paraffin-embedded tissue were placed on positively charged glass slides and pretreated by baking at 56 °C overnight. All slides were then deparaffinized by 3 immersions in xylene (Cardinal Health PN C4330) for 5 min each, followed by two 1-min immersions in 100 % alcohol (Pharmco-Aaper PN E200), two 1-min immersions in 95 % alcohol (Pharmco-Aaper PN E190), and a final 5-min immersion in molecular-grade distilled water. Slides were heated to 95 °C for 40 min and allowed to cool for 20 min at room temperature (RT). Slides were rinsed 3 times for 5 min each in distilled water. A volume of 150 μL of ProK (Dako S3020) was added to each slide and incubated for 5 min at RT. Slides were rinsed 3 times for 5 min each in distilled water. Slides were dehydrated by placing them in 95 % dehydrant alcohol (Cardinal PN C4405-12) at RT, 2 times for 1 min each, followed by placing the slides in 100 % dehydrant alcohol (Cardinal PN C4405-10) at RT for 1 min. Slides were placed on a prewarmed slide warmer at 37 °C. The probe (5 μL) (Vysis LSI ETV6) was applied to the center of the tissue and covered with a coverslip and sealed at the edges

with rubber cement. Slides were placed into the humidified HyBrite (Abbott Molecular Inc., Abbott Park, IL). The slides were denatured in the HyBrite for 5 min at 73 °C, followed by hybridization for 18 h at 37 °C. The rubber cement was removed from the hybridized slides, and they were then immersed in 2 × SSC (Vysis PN 32-804850) at RT for 5 min. Coverslips were removed, and slides were washed with 0.4 × SSC/0.3 % NP-40 (Vysis PN 32-804850, Vysis PN 32-804818) at 73 °C for 2 min. The slides were washed for 30 s at RT in 2 × SSC/0/1 % NP-40 and then air dried. One drop of VectaSheild with DAPI (Vector Labs PN H-1200) was applied to the target area of the slide. A coverslip was placed and sealed with rubber cement.

Tissue from a cellular congenital mesoblastic nephroma case was used as a positive control. Interphase nuclei were scored using a fluorescence microscope and ×150 glycerin immersion lens. A total of 100 cells were scored as "intact" or "disrupted." To avoid false positives resulting from nuclear truncation occurring in a subset of cells in paraffin-embedded samples, only tumor nuclei with all four signals present were evaluated, and overlapping cells indistinguishable as separate nuclei were excluded from the analysis. A tumor was considered rearranged for the specific gene if >10 % of tumor cells showed disrupted *ETV6*. In negative cases, the FISH was repeated and morphologic review was performed to ascertain any features that were distinctly different from the other FISH positive cases that would confer an alternative diagnosis.

Results

Of the 19 MASCs, 12 patients were female and 7 were male. The mean age was 45 years (range 16–76 years). Sixteen cases were located in the parotid gland, 2 in the submandibular gland and 1 within a periparotid lymph node. Tumor size and clinical follow-up was unknown for the majority of cases. The single in-house (case 2) occurred in a 23-year-old female; the tumor presented as a palpable mass and a fine-needle aspirate was performed prior to resection. The fine-needle aspirate was diagnosed as a low grade salivary gland neoplasm with a differential diagnosis of polymorphous low grade adenocarcinoma or mucoepidermoid carcinoma. The patient subsequently underwent a right superficial parotidectomy, the tumor measured 1.2 cm and the patient has had no evidence of disease recurrence in the past 2.5 years.

The histomorphologic features of all 19 cases are detailed in Table 1. The majority of tumors were well-circumscribed with lobules of tumor divided and surrounded by bands of fibrosis. A single tumor, although mostly well-circumscribed, demonstrated focal areas of infiltration into the adjacent parotid gland parenchyma. Four tumors (cases 4, 13, 17 and 19), also demonstrated significant desmoplasia surrounding tumor nests both in the center and at the periphery of the tumor (Fig. 1). Five tumors (cases 6, 7, 10, 14 and 15) presented as cystic lesions filled with friable tumor with a thick fibrous cyst wall; tumor nests often focally extended through the cyst wall and into the surrounding normal salivary gland parenchyma (Fig. 2). Three tumors (cases 5, 6 and 7) were bordered by a cuff of lymphocytes but did not demonstrate significant tumor infiltrating lymphocytes. Two tumors (cases 16 and 17) had both a cuff of lymphocytes as well as significant tumor infiltrating lymphocytes (Fig. 3a).

Excluding the single case that presented as a periparotid lymph node metastasis, all other cases lacked lymphovascular space invasion. Perineural invasion was seen in four cases (Fig. 3b). The mitotic rate was overall low, ranging from 0 to 2 mitotic figures per 10 high power fields. Necrosis was not seen. Three tumors (cases 1, 7 and 8) demonstrated tumor islands associated with small to medium-sized ducts; whether this represented cancerization of ducts or tumor arising from these ducts is unclear (Fig. 2). All cases demonstrated two or more architectural patterns with microcystic and solid patterns often occurring together (Fig. 4). Macrocysts were common and a single tumor presented as a single well-circumscribed nodule that was composed almost entirely of macrocysts (case 12) and looked very similar to an adenomatous thyroid nodule.

The cytologic features were similar from case to case. All tumors demonstrated some proportion of tumor cells with round nuclei with vesicular to finely granular chromatin with a single, distinct nucleolus (Fig. 5a). Moderate pleomorphism was seen in a single tumor (case 18), but most cases had only mild nuclear atypia with fairly monomorphic cytology. Cases 15 and 18 had occasional binucleate cells (Fig. 5b). In cases with papillary and pseudopapillary patterns, hobnailing of nuclei was often seen (Fig. 5c). The nuclear membranes of the majority of tumor cells were smooth, but nuclear irregularities were prominent in two tumors. Tumor cell cytoplasm was lightly eosinophilic and vacuolated. The degree of vacuolation varied from case to case, with some cases being heavily vacuolated and others demonstrating only focal vacuolation. Fine cytoplasmic granularity was occasionally seen, however, the coarse zymogen-type granules seen in serous acinic cells were not present in any of the tumors. Secretions were present in all tumors, and varied in color from light grey to light pink; some tumors had thicker, colloid-like secretions.

The immunohistochemistry results for all 19 cases are listed in Table 2. All 19 cases demonstrated diffuse expression of S100 protein and the majority demonstrated moderate to strong nuclear and cytoplasmic

Table 1 Histologic features of the nineteen putative mammary analogue secretory carcinomas

Case	Pt age (years)	Sex	Tumor location	Tumor configuration	Architecture	Nuclei	Chromatin	Nucleoli	Cytoplasm	Secretions	Other
1	43	F	Submandibular, left	Well-circumscribed, lobules with fibrous bands	Microcystic, tubular and solid	Round	Vesicular	Single, distinct	Vacuolated, lightly eosinophilic	Dense, colloid-like	Focal association with ducts
2	23	F	Parotid, right	Well-circumscribed with surrounding fibrosis	Microcystic and pseudopapillary	Oval to round, some with nuclear irregularities	Finely granular	Variably prominent	Vacuolated, lightly eosinophilic	Light pink and grey	
3	34	F	Periparotid lymph node	Multiple foci within lymph node, largest focus surrounded by fibrosis	Microcystic, macrocystic, solid and papillary	Round	Vesicular	Single, distinct	Vacuolated, eosinophilic	Light pink	
4	76	F	Parotid, right	Well-circumscribed, lobules with fibrous bands	Microcystic, macrocystic and papillary	Round	Vesicular	Single, distinct	Vacuolated, lightly eosinophilic	Light pink and grey to colloid-like	Focal cuff of lymphocytic inflammation, desmoplasia surrounding tumor islands within the tumor
5	71	M	Parotid, right	Well-circumscribed with surrounding fibrosis	Microcystic and macrocystic	Round	Vesicular	Single, distinct	Vacuolated, eosinophilic	Pink to colloid-like	Focal cuff of lymphocytic inflammation
6	55	F	Parotid, right	Cystic lesion with fibrous wall	Macrocystic and solid	Round	Finely granular	Single, distinct	Vacuolated, eosinophilic	Light pink and grey	Focal cuff of lymphocytic inflammation
7	16	F	Parotid, right	Cystic lesion with fibrous wall	Microcystic and solid	Oval to round	Finely granular and vesicular	Single, distinct	Eosinophilic	Light grey	Association with ducts and focal cuff of lymphocytic inflammation
8	22	M	Parotid, right	Well-circumscribed, lobules with fibrous bands	Microcystic, macrocystic and solid	Round	Vesicular	Single, distinct	Heavily vacuolated, lightly eosinophilic	Light pink and grey	Focal association with ducts
9	26	M	Parotid, right	Well-circumscribed, multicystic lesion with dividing bands of fibrosis	Predominantly papillary and pseudopapillary with focal microcystic areas	Round with focal hobnailing	Finely granular and vesicular	Single, distinct	Eosinophilic	Focal, light pink to grey	

Table 1 continued

Case	Pt age (years)	Sex	Tumor location	Tumor configuration	Architecture	Nuclei	Chromatin	Nucleoli	Cytoplasm	Secretions	Other
10	56	M	Parotid, right	Cystic lesion with fibrous wall	Papillary, microcystic and macrocystic	Round with focal hobnailing	Finely granular and vesicular	Single, distinct	Eosinophilic, focally vacuolated	Light pink	
11	45	F	Parotid, left	Well-circumscribed with surrounding fibrosis	Microcystic, macrocystic and focally pseudopapillary	Round	Vesicular	Single, distinct	Heavily vacuolated, lightly eosinophilic	Light pink	
12	37	F	Parotid, left	Well-circumscribed with surrounding fibrosis	Macrocystic and focally microcystic	Round	Finely granular	Single, distinct	Lightly eosinophilic, focally vacuolated	Pink to colloid-like	Similar pattern to an adenomatous thyroid nodule
13	53	M	Parotid, nos	Well-circumscribed, lobules with fibrous bands	Microcystic and solid	Round, some with nuclear irregularities	Vesicular	Single, distinct	Heavily vacuolated, lightly eosinophilic	Light grey	Desmoplasia surrounding tumor islands within the tumor
14	46	F	Parotid, left	Cystic lesion with fibrous wall	Microcystic and solid	Round	Vesicular	Single, distinct	Vacuolated, eosinophilic	Light pink and grey	
15	56	M	Parotid, right	Cystic lesion with fibrous wall	Microcystic, macrocystic, papillary and pseudopapillary	Round with focal hobnailing	Vesicular	Single, distinct	Vacuolated, eosinophilic	Light pink to colloid-like	Occasional binucleate cells
16	28	F	Parotid, right	Well-circumscribed, lobules with fibrosis	Microcystic, tubular and solid	Round	Vesicular	Single, distinct	Vacuolated, eosinophilic	Light pink and grey, focally colloid-like	Surrounding lymphocytic inflammation with tumor infiltrating lymphocytes
17	unk	F	Parotid, right	Mostly well-circumscribed, focally infiltrative, lobules with fibrosis	Microcystic, tubular and solid	Round	Vesicular	Single, distinct	Vacuolated, eosinophilic	Light pink, colloid-like	Desmoplasia surrounding tumor islands, surrounding lymphocytic inflammation with tumor infiltrating lymphocytes
18	66	F	Parotid, left	Well-circumscribed with surrounding fibrosis	Microcystic and solid	Oval to round, some with nuclear irregularities	Finely granular and vesicular	Single distinct	Vacuolated, eosinophilic	Light pink	Moderate cytologic pleomorphism, rare cells with binucleation

Table 1 continued

Case	Pt age (years)	Sex	Tumor location	Tumor configuration	Architecture	Nuclei	Chromatin	Nucleoli	Cytoplasm	Secretions	Other
19	53	M	Submandibular, right	Well-circumscribed, lobules with fibrosis	Microcystic, macrocystic, tubular and solid	Round	Finely granular and vesicular	Single, distinct	Vacuolated, eosinophilic	Light grey	Desmoplasia surrounding tumor islands within the tumor

unk unkown, *M* male, *F* female

staining intensity (Fig. 6a). Strong and diffuse mammaglobin expression was seen in 18 of 19 (95 %) of cases (Fig. 6b). A single tumor (case 8) demonstrated very rare, scattered expression of mammaglobin in both the secretions and tumor cells (Fig. 6c). The S100 protein expression in this case was diffuse but of moderate nuclear and cytoplasmic intensity. Diffuse and strong vimentin and cytokeratin expression was seen in all cases in which it was performed (9 of 9 cases, 100 % and 11 of 11 cases, 100 %, respectively). Cytokeratin expression included staining for either AE1/AE3, CAM5.2, CK7 or CK19. Although p63 and/or SMA were performed in only 7 cases, all cases lacked expression of these markers. BRST-2 expression was seen in approximately one-third of cases tested (4 of 11, 36 %).

Eighteen of 19 cases (95 %) (including case 8 with the "rare" mammaglobin expression) demonstrated the *ETV6* rearrangement by fluorescence in situ hybridization (Fig. 7a).

A single tumor (case 7) was negative for the *ETV6* rearrangement. This tumor was largely composed of a single cystic mass with tumor cells lining and infiltrating the fibrous cyst wall. The architecture of the tumor was predominantly microcystic and the cytology was essentially identical to all other cases with lightly eosinophilic cytoplasm that was heavily vacuolated in some areas (Fig. 2). The tumor cell nuclei were round with vesicular chromatin and a single distinct nucleolus, often centrally located was seen. Immunohistochemistry for DOG1 was performed on this case and was negative. No particular morphologic feature that departed from any of the other cases was apparent and despite the negative *ETV6* we believe the best classification for this tumor is a MASC.

The single low-grade cribriform cystadenocarcinoma, like the 19 MASCs demonstrated expression of S100 protein and mammaglobin; however, *ETV6* was intact. This tumor was a cystic lesion that contained a dense fibrous wall as well as well-rounded nests of tumor cells within the fibrous wall and the parotid gland parenchyma. Microcystic and solid architectural patterns were seen within the well-rounded tumor nests. The slit-like microcystic areas contained light pink secretions. The tumor cell nuclei were oval with smooth, finely granular chromatin with small to medium, distinct nucleoli that were often eccentrically placed (Fig. 8). The cytoplasm was eosinophilic and lacked vacuolation. Cell membranes were very distinct with sharp outlines, a feature not seen in any of the MASCs. While architecturally there were similarities to MASC, the overall morphology was reminiscent of a ductal hyperplasia or ductal carcinoma in situ, thus supporting its reclassification as a low-grade cribriform cystadenocarcinoma.

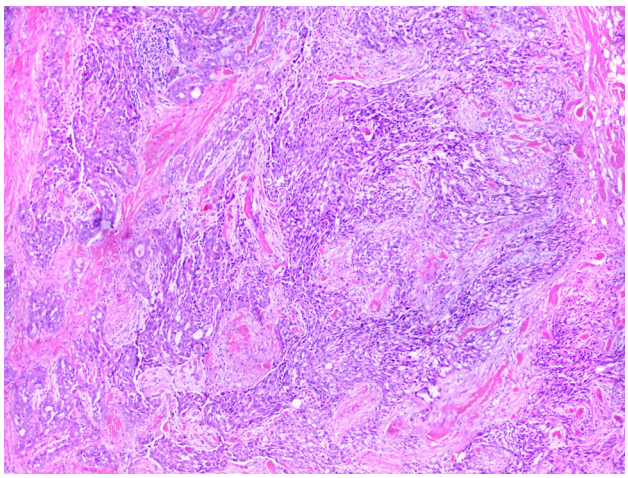

Fig. 1 Four tumors, including this one (case 17), demonstrated islands of tumor cells with surrounding desmoplasia (H&E, 10×)

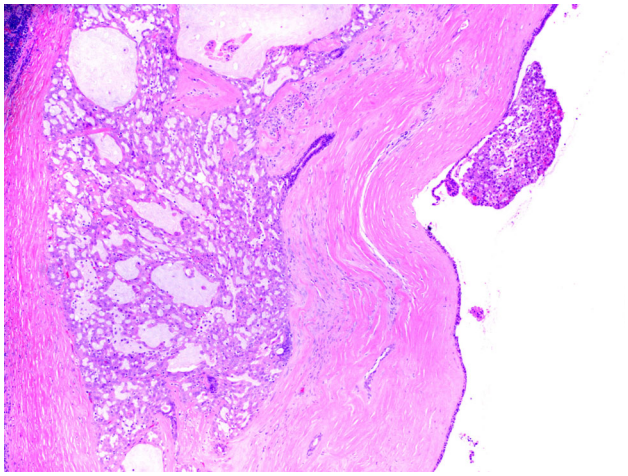

Fig. 2 This tumor (case 7) is predominantly a cystic lesion filled with friable tumor. There are tumor islands that infiltrate into the fibrous cyst wall and are associated with a medium-sized duct (H&E, 4×)

Discussion

In 2010, Skalova et al. [1] described MASC as a distinct salivary gland tumor that was molecularly, immunohistochemically and morphologically analogous to secretory carcinoma of the breast. In the past, this tumor was likely most often classified as either a zymogen granule poor acinic cell carcinoma, cystadenocarcinoma or adenocarcinoma not otherwise specified [1, 21]. Currently, molecular confirmation is considered the gold standard for the diagnosis of MASC. However, we postulated that the morphologic features together with supporting immunohistochemistry are sufficient for a diagnosis of MASC.

Despite the ongoing elaboration of new morphologic features, in our experience there are certain constant features that are characteristic of this tumor and were reported in the initial paper describing MASC [1, 21, 22]. These features include tumor cells with oval to round nuclei with vesicular to finely granular chromatin and a single distinct nucleolus. Tumor cell cytoplasm is eosinophilic and vacuolated. Architectural growth patterns are varied and include microcystic, tubular, solid, macrocystic, papillary and pseudopapillary patterns. Intraluminal secretions ranging from light pink to colloid-like is also usually present.

The majority of MASCs typically demonstrate coexpression of S100 protein and mammaglobin, although focal weak or absent expression of S100 protein has been reported in intraoral tumors [1, 22–24]. Using the above histologic features as a springboard for diagnosis as well as supporting coexpression of S100 protein and mammaglobin, we rendered a diagnosis of MASC in total of 19 consultation cases sourced from the University of Virginia and the Mount Sinai Health System-Beth Israel Medical Center. Retrospective FISH for *ETV6* was then performed on all 19 cases. In this study, we demonstrated a 95 % correlation rate with FISH when using solely morphology in conjunction with immunohistochemistry. This high percentage supports our hypothesis that morphology in conjunction with immunohistochemistry is sufficient to render a diagnosis of MASC.

It was surprising to us that case 7 was negative by FISH, as the morphologic and immunohistochemical features to our eyes were characteristic of MASC. This tumor may represent a zymogen granule poor acinic cell carcinoma; however, the strong mammaglobin expression would be at odds with this diagnosis. Additionally, the lack of DOG1 expression is more consistent with a MASC rather than a zymogen granule poor acinic cell carcinoma [20]. Chiosea et al. [21] retrospectively reviewed a series of zymogen granule poor acinic cell carcinomas. FISH for *ETV6* was performed on all 17 cases of zymogen granule poor acinic cell carcinomas and immunohistochemistry for S100 protein was performed on a subset of cases [21]. Cases that harbored the *ETV6* rearrangement were redesignated as MASC. Chiosea et al. [21] did not find striking histologic differences between MASC and the zymogen granule poor acinic cell carcinoma, but did state that MASC tended to be more solid and microcystic whereas zymogen granule poor acinic cell carcinoma had a cystic, papillary growth pattern. This study would suggest that FISH would be the best method to distinguish these two entities, but given the small series of zymogen granule poor acinic cell carcinomas as well as the lack of assessment of mammaglobin between the two entities, further comparative study is needed.

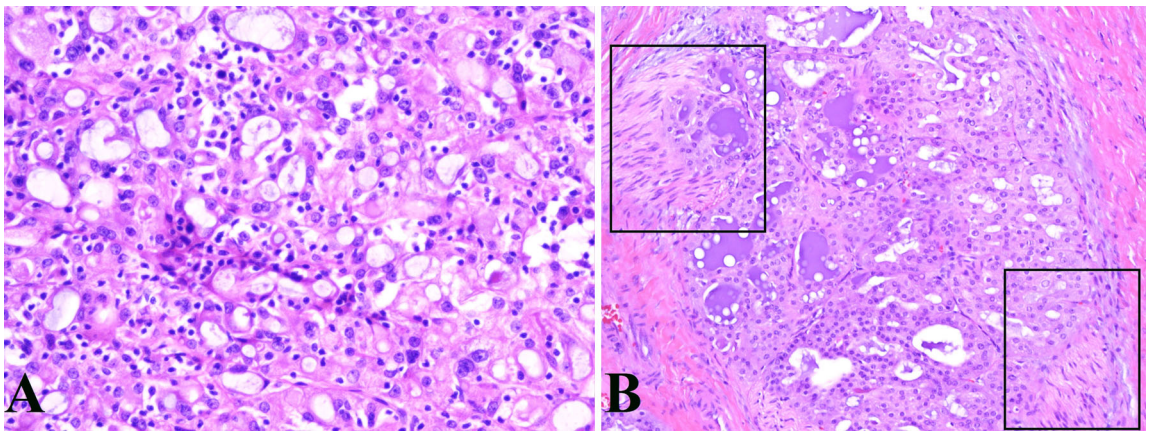

Fig. 3 **a** This tumor (case 16) demonstrates a microcystic architecture with intraluminal *light grey* secretions which represents the typical morphologic features seen in mammary analogue secretory carcinoma. In addition, this tumor also demonstrates significant tumor infiltrating lymphocytes (H&E, 20×). **b** This tumor (case 1) also demonstrates the characteristic microcystic and tubular architectural patterns of mammary analogue secretory carcinoma. Additionally, this tumor demonstrates the denser, colloid-like secretions that can sometimes be seen as well as the tumor's capacity for perineural invasion, as highlighted by the *squares* (H&E, 20)

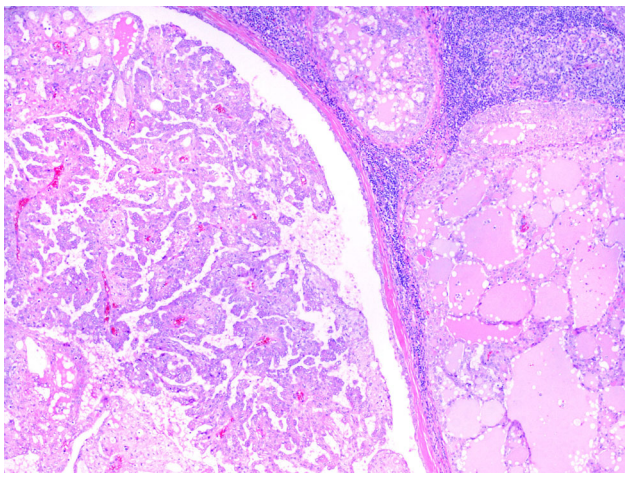

Fig. 4 This tumor (case 4) was located within a periparotid lymph node. The tumor deposits demonstrate a variety of architectural patterns including microcystic, macrocystic and papillary (H&E, 4×)

We used the combination of S100 protein and mammaglobin expression as an adjunct to the diagnosis of MASC. Patel et al. [23] have shown that polymorphous low-grade adenocarcinoma and adenoid cystic carcinoma can also demonstrate significant co-expression of these immunohistochemical markers. In our experience the histologic and cytologic features of adenoid cystic carcinoma allow its easy distinction from MASC; although, in cases with high-grade transformation molecular studies would be prudent. Recently, MASC have been described in the oral cavity [22, 24]. Given the predilection of polymorphous low-grade adenocarcinoma (PLGA) for this site, this tumor may enter the differential diagnosis. In our experience, PLGA tends to be more infiltrative as compared to the well-circumscribed MASC. Both share cytologic monotony and variable architectural patterns as well as the potential for co-expression of S100 protein and mammaglobin. However, the degree of secretions and cytoplasmic

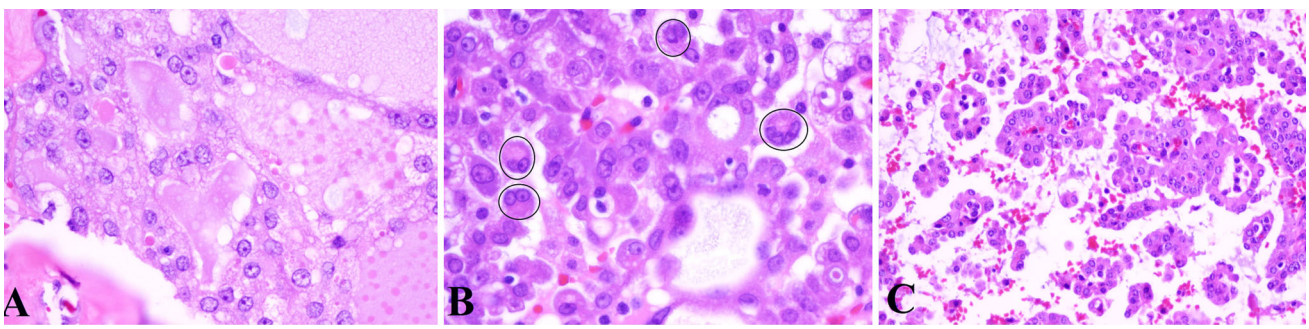

Fig. 5 a Tumor cells are characterized by oval to round nuclei with vesicular chromatin and a single, distinct nucleolus. This tumor also features cytoplasmic vacuolation (H&E, 40×). **b** Binucleate tumor cells, as highlighted by the *circles*, were occasionally seen (H&E, 40×). **c** Tumors with a pseudopapillary and papillary architecture demonstrated occasional hobnailing of nuclei (H&E, 40×)

Table 2 The immunohistochemical profile of the nineteen putative mammary analogue secretory carcinomas

Case	S100	MGB	Vim	BRST-2	CK	p63	SMA
1	+	+	+	–	nd	–	nd
2	+	+	nd	nd	nd	–	–
3	+	+	nd	–	+	–	nd
4	+	+	nd	nd	nd	nd	nd
5	+	+	nd	nd	nd	nd	nd
6	+	+	nd	nd	nd	nd	nd
7	+	+	nd	nd	+	nd	–
8	+	rare +	nd	nd	nd	nd	nd
9	+	+	nd	rare +	+	nd	–
10	+	+	nd	nd	nd	nd	nd
11	+	+	nd	nd	nd	nd	nd
12	+	+	+	rare +	+	–	nd
13	+	+	+	–	+	nd	nd
14	+	+	+	+	+	–	nd
15	+	+	+	–	+	nd	nd
16	+	+	+	+	+	nd	nd
17	+	+	+	–	+	nd	nd
18	+	+	+	–	+	nd	nd
19	+	+	+	–	+	nd	nd

+ positive staining, – negative staining, *nd* not done, S100, S100 protein, *MGB* mammaglobin, *Vim* Vimentin, *CK* cytokeratins (including AE1/AE3, CAM5.2, CK7, and/or CK19)

vacuolation seen in MASC is not typical of PLGA. Nonetheless, FISH confirmation of intraoral tumors may be helpful. Of note, while all intraoral cases of MASC reported by Bishop et al. demonstrated co-expression of S100 protein and mammaglobin, Connor et al. had focal and absent expression of S100 protein in two of four intraoral MASCs [22, 24]. These two intraoral tumors also demonstrated isolated tumor cells with nuclear p63 expression [22]. Although the majority of MASC lack expression of basal/myoepithelial markers, there are rare cases that demonstrate focal expression of p63 [25].

Mammaglobin staining in 18 cases was strong and diffuse and was present in both the tumor cell cytoplasm and intraluminal secretions. A single tumor (case 8) demonstrated very rare yet strong cellular mammaglobin expression; given the overall morphology we classified this tumor as a MASC. The majority of the literature suggests that staining for mammaglobin in MASCs is typically diffuse; the rare expression seen in case 8 may be due to differences in fixation as this was a consultation case [26]. Alternatively, mammaglobin may be only focally expressed in some MASCs as is the case with many invasive breast cancers [27].

In our initial morphologic review, we did have a single case that was reclassified as a low-grade cribriform cystadenocarcinoma, also known as a low-grade salivary duct carcinoma and intraductal carcinoma. Both MASC and low-grade cribriform cystadenocarcinoma have overlapping morphologic features particularly in their architectural patterns and the presence of secretions. Additionally, both tumors typically demonstrate expression of S100 protein and a single case of low-grade cribriform cystadenocarcinoma has been previously shown to demonstrate mammaglobin expression [26, 28]. This study adds another mammaglobin expressing low-grade cribriform cystadenocarcinoma to the literature. In their initial paper on MASC, Skalova et al. [1] did study a single case of a low-grade cribriform cystadenocarcinoma which was negative for the *ETV6* rearrangement, and the low-grade cribriform cystadenocarcinoma in this study was also negative for the ETV6 rearrangement suggesting that these tumors are distinct entities. However, the rarity of low-grade cribriform cystadenocarcinoma makes a comparative study between these two tumors difficult, and it remains to be seen whether this pathologic distinction is even clinically relevant.

There are some histologic features that were noted during our review that have not been previously highlighted. Some of our tumors featured desmoplasia

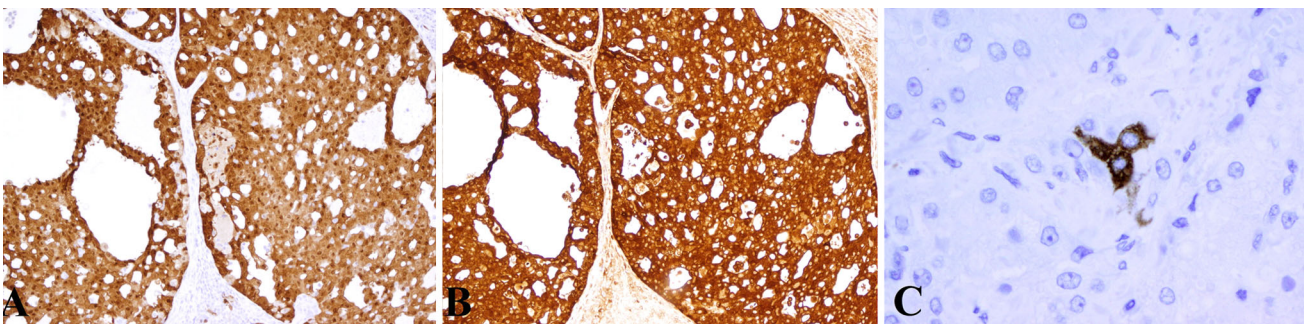

Fig. 6 **a** All tumors demonstrated moderate to strong nuclear and cytoplasmic expression of S100 protein (H&E, 10×). **b** Eighteen tumors demonstrated strong cytoplasmic expression of mammaglobin (H&E, 10×). **c** A single tumor (case 8) demonstrated very rare expression of mammaglobin in tumor cells and secretions (H&E, 40×)

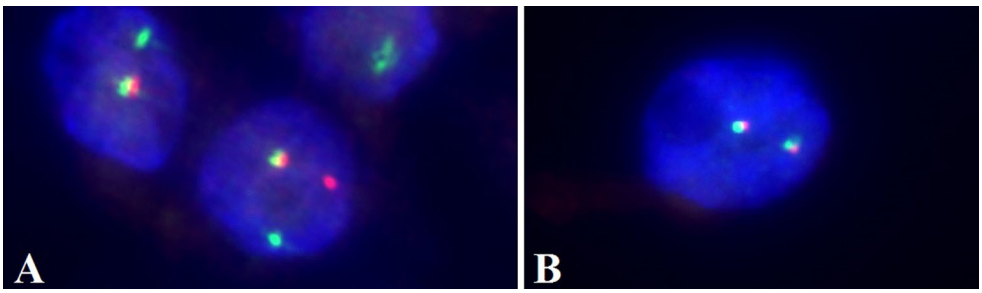

Fig. 7 Fluorescence in situ hybridization with the Vysis LSI ETV6 probe. **a** Interphase nuclei demonstrating a disrupted *ETV6* signal (glycerin immersion, 150×). **b** Interphase nuclei demonstrating an intact *ETV6* signal (glycerin immersion, 150×)

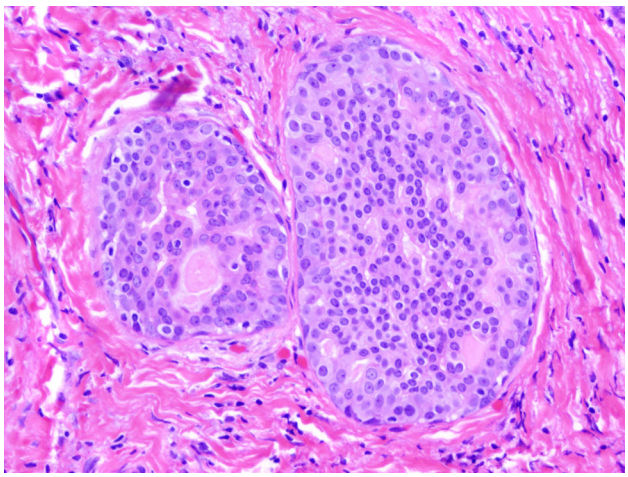

Fig. 8 This tumor was reclassified as a low-grade cribriform cystadenocarcinoma also known as low-grade salivary duct carcinoma and intraductal carcinoma. The cytologic and architectural features were unconventional when compared to the 19 MASCs in this series. This tumor featured well-rounded tumor nests that contained tumor cells with oval nuclei, finely granular chromatin and eccentric nucleoli. The tumor cell cytoplasm is eosinophilic but lacks vacuolation and minimal secretions are present. The tumor cells have distinct cell borders, a feature not seen in MASC (H&E, 20×)

surrounding tumor nests. Despite the desmoplasia, the tumors remained well-circumscribed. A cuff of lymphocytic infiltrate was seen in 5 cases and two of these cases had tumor infiltrating lymphocytes. With regards to cytology, although the majority of tumor cells were round and atypia was usually mild, there were two cases that demonstrated binucleation and a single case with moderate pleomorphism. Hobnailing of tumor nuclei has been previously reported and was also seen in this study specifically in cases with papillary and pseudopapillary architectural growth patterns [22].

As previously reported, we also observed tumor cells associated with ducts in three cases [22]. The significance of this finding is unclear [22]. Except for case 3 which presented as a lymph node metastasis, lymphovascular invasion was not a typical finding. Perineural invasion was seen in four cases, however, necrosis was absent in all cases and the tumors had very low mitotic rates. In most published series, MASCs have tended to predominate in men; however, in our cohort that majority occurred in women [1, 22, 29]. Like the prior studies, our patient age range was wide [1, 22].

In our consult services, we have noticed the increased frequency of accurate histomorphologic identification of MASC by our referring pathologists. Given that molecular studies are not routinely available in these smaller academic or private practice groups from which the majority of our cases are sourced, the requirement of molecular confirmation in order to diagnosis MASC needs to be addressed. This study has shown that the majority of tumors (95 %) can be accurately classified as MASC based solely on morphology and immunohistochemistry. However, we do concede that in cases with atypical features or with areas of high-grade transformation, molecular confirmation should be performed. There are very limited studies detailing the behavior of MASCs; one study suggested there was a slight increase of lymph node metastasis when compared to acinic cell carcinomas [29]. Although the majority of MASCs appear to behave as low-grade malignancies, there is a real risk of high-grade transformation, local recurrence, lymph node and distant metastasis and even death in rare cases [1, 30]. With the growing armamentarium of molecular-based targeted therapies it is foreseeable that in the future the subset of tumors with high-grade transformation may benefit from such therapy and confirmatory molecular testing may be necessary.

Acknowledgments Special thanks to Harriet Scruggs for allowing us to use her laboratory expertise in fluorescence in situ hybridization.

Conflict of interest No conflicts of interest.

References

1. Skalova A, Vanecek T, Sima R, Laco J, Weinreb I, Perez-Ordonez B, Starek I, Geierova M, Simpson RH, Passador-Santos F, Ryska A, Leivo I, Kinkor Z, Michal M. Mammary analogue

secretory carcinoma of salivary glands, containing the ETV6-NTRK3 fusion gene: a hitherto undescribed salivary gland tumor entity. Am J Surg Pathol. 2010;34:599–608.
2. Tognon C, Knezevich SR, Huntsman D, Roskelley CD, Melnyk N, Mathers JA, Becker L, Carneiro F, MacPherson N, Horsman D, Poremba C, Sorensen PH. Expression of the ETV6-NTRK3 gene fusion as a primary event in human secretory breast carcinoma. Cancer Cell. 2002;2:367–76.
3. Knezevich SR, McFadden DE, Tao W, Lim JF, Sorensen PH. A novel ETV6-NTRK3 gene fusion in congenital fibrosarcoma. Nat Genet. 1998;18:184–7.
4. Rubin BP, Chen CJ, Morgan TW, Xiao S, Grier HE, Kozakewich HP, Perez-Atayde AR, Fletcher JA. Congenital mesoblastic nephroma t(12;15) is associated with ETV6-NTRK3 gene fusion: cytogenetic and molecular relationship to congenital (infantile) fibrosarcoma. Am J Pathol. 1998;153:1451–8.
5. Eguchi M, Eguchi-Ishimae M, Tojo A, Morishita K, Suzuki K, Sato Y, Kudoh S, Tanaka K, Setoyama M, Nagamura F, Asano S, Kamada N. Fusion of ETV6 to neurotrophin-3 receptor TRKC in acute myeloid leukemia with t(12;15)(p13;q25). Blood. 1999;93:1355–63.
6. Kralik JM, Kranewitter W, Boesmueller H, Marschon R, Tschurtschenthaler G, Rumpold H, Wiesinger K, Erdel M, Petzer AL, Webersinke G. Characterization of a newly identified ETV6-NTRK3 fusion transcript in acute myeloid leukemia. Diagn Pathol. 2011;6:19.
7. Lannon CL, Sorensen PH. ETV6-NTRK3: a chimeric protein tyrosine kinase with transformation activity in multiple cell lineages. Semin Cancer Biol. 2005;15:215–23.
8. Nordkvist A, Mark J, Gustafsson H, Bang G, Stenman G. Non-random chromosome rearrangements in adenoid cystic carcinoma of the salivary glands. Genes Chromosomes Cancer. 1994;10:115–21.
9. Mitani Y, Li J, Rao P, Zhao YJ, Bell D, Lippman SM, Weber RS, Caulin C, El-Naggar AK. Comprehensive analysis of the MYB-NFIB gene fusion in salivary adenoid cystic carcinoma: incidence, variability, and clinicopathologic significance. Clin Cancer Res. 2010;16:4722–31.
10. Brill LB, Kanner WA, Fehr A, Andrén Y, Moskaluk CA, Löning T, Stenman G, Frierson HF Jr. Analysis of MYB expression and MYB-NFIB gene fusions in adenoid cystic carcinoma and other salivary neoplasms. Mod Pathol. 2011;24:1169–76.
11. Martins C, Cavaco B, Tonon G, Kaye FJ, Soares J, Fonseca I. A study of MECT1-MAML2 in mucoepidermoid carcinoma and Warthin's tumor of salivary glands. J Mol Diagn. 2004;6:205–10.
12. Behboudi A, Enlund F, Winnes M, Andrén Y, Nordkvist A, Leivo I, Flaberg E, Szekely L, Mäkitie A, Grenman R, Mark J, Stenman G. Molecular classification of mucoepidermoid carcinomas-prognostic significance of the MECT1-MAML2 fusion oncogene. Genes Chromosomes Cancer. 2006;45:470–81.
13. Kas K, Voz ML, Röijer E, Aström AK, Meyen E, Stenman G, Van de Ven WJ. Promoter swapping between the genes for a novel zinc finger protein and beta-catenin in pleiomorphic adenomas with t(3;8)(p21;q12) translocations. Nat Genet. 1997;15:170–4.
14. Kas K, Voz ML, Hensen K, Meyen E, Van de Ven WJ. Transcriptional activation capacity of the novel PLAG family of zinc finger proteins. J Biol Chem. 1998;273:23026–32.
15. Astrom AK, Voz ML, Kas K, Röijer E, Wedell B, Mandahl N, Van de Ven W, Mark J, Stenman G. Conserved mechanism of PLAG1 activation in salivary gland tumors with and without chromosome 8q12 abnormalities: identification of SII as a new fusion partner gene. Cancer Res. 1999;59:918–23.
16. Persson F, Andren Y, Winnes M, Wedell B, Nordkvist A, Gudnadottir G, Dahlenfors R, Sjögren H, Mark J, Stenman G. High-resolution genomic profiling of adenomas and carcinomas of the salivary glands reveals amplification, rearrangement, and fusion of HMGA2. Genes Chromosomes Cancer. 2009;48:69–82.
17. Matsuyama A, Hisaoka M, Nagao Y, Hashimoto H. Aberrant PLAG1 expression in pleomorphic adenomas of the salivary gland: a molecular genetic and immunohistochemical study. Virchows Arch. 2011;458:583–92.
18. Antonescu CR, Katabi N, Zhang L, Sung YS, Seethala RR, Jordan RC, Perez-Ordoñez B, Have C, Asa SL, Leong IT, Bradley G, Klieb H, Weinreb I. EWSR1-ATF1 fusion is a novel and consistent finding in hyalinizing clear-cell carcinoma of salivary gland. Genes Chromosomes Cancer. 2011;50:559–70.
19. Shah AA, LeGallo RD, van Zante A, Frierson HF Jr, Mills SE, Berean KW, Mentrikoski MJ, Stelow EB. EWSR1 genetic rearrangements in salivary gland tumors: a specific and very common feature of hyalinizing clear cell carcinoma. Am J Surg Pathol. 2013;37:571–8.
20. Chenevert J, Duvvuri U, Chiosea S, Dacic S, Cieply K, Kim J, Shiwarski D, Seethala RR. DOG1: a novel marker of salivary acinar and intercalated duct differentiation. Mod Pathol. 2012;25:919–29.
21. Chiosea SI, Griffith C, Assaad A, Seethala RR. The profile of acinic cell carcinoma after recognition of mammary analog secretory carcinoma. Am J Surg Pathol. 2012;36:343–50.
22. Connor A, Perez-Ordonez B, Shago M, Skalova A, Weinreb I. Mammary analog secretory carcinoma of salivary gland origin with the ETV6 gene rearrangement by FISH: expanded morphologic and immunohistochemical spectrum of a recently described entity. Am J Surg Pathol. 2012;36(1):27–34.
23. Patel KR, Solomon IH, El-Mofty SK, Lewis JS Jr, Chernock RD. Mammaglobin and S-100 immunoreactivity in salivary gland carcinomas other than mammary analogue secretory carcinoma. Hum Pathol. 2013;44:2501–8.
24. Bishop JA, Yonescu R, Batista D, Eisele DW, Westra WH. Most nonparotid "acinic cell carcinomas" represent mammary analog secretory carcinomas. Am J Surg Pathol. 2013;37:1053–7.
25. Laco J, Svajdler M Jr, Andrejs J, Hrubala D, Hacova M, Vanacek T, Skalova A, Ryska A. Mammary analog secretory carcinoma of salivary glands: a report of 2 cases with expression of basal/myoepithelial markers (calponin, CD10 and p63 protein). Pathol Res Pract. 2013;209:167–72.
26. Bishop JA, Yonescu R, Batista D, Begum S, Eisele DW, Westra WH. Utility of mammaglobin immunohistochemistry as a proxy marker for the ETV6-NTRK3 translocation in the diagnosis of salivary mammary analogue secretory carcinoma. Hum Pathol. 2013;44:1982–8.
27. Sasaki E, Tsunoda N, Hatanaka Y, Mori N, Iwata H, Yatabe Y. Breast-specific expression of MGB1/mammaglobin: an examination of 480 tumors from various organs and clinicopathological analysis of MGB1-positive breast cancers. Mod Pathol. 2007;20:208–14.
28. Brandwein-Gensler M, Hille J, Wang BY, Urken M, Gordon R, Wang LJ, Simpson JR, Simpson RH, Gnepp DR. Low-grade salivary duct carcinoma: description of 16 cases. Am J Surg Pathol. 2004;28:1040–4.
29. Chiosea SI, Griffith C, Assaad A, Seethala RR. Clinicopathological characterization of mammary analogue secretory carcinoma of salivary glands. Histopathology. 2012;61:387–94.
30. Skalova A, Vanecek T, Majewska H, Laco J, Grossmann P, Simpson RH, Hauer L, Andrle P, Hosticka L, Branzovsky J, Michal M. Mammary analogue secretory carcinoma of salivary glands with high-grade transformation: report of 3 cases with the ETV6-NTRK3 gene fusion and analysis of TP53, β-catenin, EGFR, and CCND1 genes. Am J Surg Pathol. 2014;38:23–33.